

SOME EXPERIMENTAL STUDIES
OF
LAMINAR BURNING VELOCITY

Thesis by
Lt. Herbert "R" Poorman, U.S.N.

In Partial Fulfillment of the Requirements
for the Degree of
Aeronautical Engineer

California Institute of Technology
Pasadena, California

1953

ACKNOWLEDGEMENT

The author is indebted to Dr. S. S. Penner for initiating this study, for his helpful suggestions throughout the course of the work, and for his assistance in interpreting the results.

The author also wishes to express his appreciation to Mrs. Elizabeth Fox for typing the thesis.

ABSTRACT

One of the important physical parameters in flame propagation is the laminar burning velocity. A great many experimental measurements of the burning velocity have been made using a variety of experimental techniques. Furthermore, the problem has been studied theoretically by a number of different investigators. Extensive references to the original literature may be found in the books by Lewis and von Elbe⁽¹⁾ and by Jost⁽²⁾.

This thesis is concerned with experimental studies of flame propagation in acetylene-oxygen systems containing the inert gases argon, carbon dioxide, helium, and nitrogen. These studies are introduced with a survey of experimental techniques for measuring the laminar burning velocity in premixed gases. Next, some new experimental measurements obtained by use of a small burner tube at atmospheric pressure are described. The new data are interpreted qualitatively by utilizing a thermal theory of laminar flame propagation.

TABLE OF CONTENTS

PART	PAGE
I SURVEY OF EXPERIMENTAL TECHNIQUES FOR MEASURING LAMINAR BURNING VELOCITY IN PREMIXED GASES	
Introduction	1
A. Definitions of Laminar Burning Velocity	1
B. Historical Survey of Flame Speed Measurement on Flames Formed on Burner Tubes	2
C. Selection of Method for Measuring Flame Velocity on Burner Tubes	5
D. Other Methods for Measuring the Laminar Burning Velocity	11
1. The Flat Flame Method	11
2. The Soap Bubble or Constant-Pressure Method	12
3. The Spherical Bomb or Constant-Volume Method	15
II. APPARATUS AND EXPERIMENTAL TECHNIQUE	17
III. EXPERIMENTAL RESULTS AND DISCUSSION	20
REFERENCES	40
LIST OF FIGURES	42

EXPERIMENTAL STUDIES OF LAMINAR BURNING VELOCITY IN PREMIXED GASES

I. SURVEY OF EXPERIMENTAL TECHNIQUES FOR MEASURING LAMINAR BURNING VELOCITY IN PREMIXED GASES

It seems appropriate to introduce experimental studies on laminar flame propagation with a precise definition of the burning velocity. This introduction is followed by a brief historical summary of methods used for measuring the laminar flame velocity in approximately conical burner flames. On the basis of published data relating to experimental measurements, and recent investigations relating to burner flames, some justification will be given for the method used in this work for determining the burning velocity.

A. Definition of Laminar Burning Velocity

The laminar burning velocity (which is used synonymously with flame speed, burning velocity, rate of propagation of a combustion wave, and fundamental flame speed) is defined as the velocity of the reaction zone front with respect to the unburnt gas⁽¹⁾. Consider the stream tube 1 (Cf. Fig. 1) passing through the area elements dA_1 and dA_2 where dA_1 is normal to the axis of the tube. Assume the axial component of the flow velocity, U_u , is constant across dA_1 , and also assume that steady state conditions exist. The surface T_1 is the reaction front, and dA_2 lies in this surface. The fictitious stream tube 2 passes through dA_2 and dA_2' , where dA_2 and dA_2' are perpendicular to the axis of tube 2.

Application of the equation of conservation of mass to tube 1 gives

$$\rho_u U_u dA_1 = \rho_1 U_1 dA_2 \quad (1)$$

where U_1 is defined as the axial component of velocity in tube 2 and is assumed to be uniform across the tube. From the definition of burning velocity it follows that

$$\rho_1 U_1 dA_2 = \rho_u U_b dA_2 \quad (2)$$

where U_b represents the normal burning velocity. Combining Equations (1) and (2) gives the result

$$U_b = U_u (dA_1/dA_2) = U_1 (\rho_1/\rho_u) \quad (3)$$

It should be noted that U_1 is the actual normal velocity of the flame front with respect to the unburnt gas mixture immediately ahead of the front while U_b is the velocity of the flame front with respect to the cold gas, i. e., with respect to the initial combustible mixture.

B. Historical Survey of Flame Speed Measurements on Flames Formed on Burner Tubes

The first burning velocity measurements were made by Bunsen⁽³⁾ who assumed that the downward velocity of the flame front just exceeded the upward velocity of the gas mixture at the point of flashback. Bunsen's method would be expected to yield significant data only if the flow velocity were uniform across the burner tube, which is, of course, not the case in fully developed laminar flow.

Gouy⁽⁴⁾ first considered the flame speed to be equal to the product of the gas velocity and the sine of the angle which the flame cone makes with the axis of the burner tube. When Gouy found that

the surface formed by the flame front did not approximate sufficiently closely to a true cone, and that the results obtained depended upon the position on the flame front at which the angle was measured, he eliminated the angle from consideration by setting the flame speed equal to the volume rate of flow of the mixture divided by the area of the flame surface. Gouy determined the area of the flame surface by measurement on a real image of the flame formed by use of a suitable optical system. He considered the boundary of the image as the projection of a surface of revolution and then obtained the area by integration.*

Michelson⁽⁵⁾ used the same principle as Gouy but employed enlarged photographs of the image to facilitate study and analysis of the flame surface.

Ubbelohde and Koelliker⁽⁶⁾ concluded that the rounded tip and the curved base of the flame surface indicate distortions which should be eliminated in the determination of normal burning velocity. Consequently, they measured the angle at the "straight" portion of the conical surface and computed the normal burning velocity by using essentially Gouy's original method.

Stevens⁽⁷⁾ showed that burning velocities obtained by use of the Bunsen-type burner flames, measuring the area of a flame surface as had been done by Gouy, Michelson, and Ubbelohde, did not agree satisfactorily with the results he obtained using the soap bubble method (Cf. Section I-D for a description of this technique). He reasoned that the approximately conical flame surface was the result of -----

*Note: See Fig. 2 for the basic geometrical relation between a conical flame and its projected triangular image.

several factors, one of which was a velocity profile across the burner tube which varied from zero at the walls to a maximum at the center. Stevens therefore tried to make use of only the part of the flame surface which resulted from that portion of the gas mixture whose linear velocity upon leaving the port was equal to the mean velocity in the tube. His method for accomplishing the desired results was essentially the same as the one used in the present studies, which is discussed in some detail in Section I-C. The same method has been used also by Smith and Pickering⁽⁸⁾.

Smith⁽⁹⁾ conducted a rather extensive literature survey, summarized the influence of experimental factors on the numerical results obtained for the laminar burning velocity by the use of various burner tube methods, and reached the following conclusions:

- (1) The numerical value of U_b is independent of U_u as long as the flow is laminar. Ubbelohde and Koclikier⁽⁶⁾ were among the first investigators to establish this result, which has since been confirmed repeatedly.
- (2) The apparent value of U_b depends upon the size of the burner port, especially if the area of the flame is used in obtaining the burning velocity. This phenomenon is referred to as the "quenching effect" and is associated with heat transfer to the tube. The problem of flame quenching has been studied by many different investigators. It is clear that the influence of the burner size can be minimized by using burner tubes of large diameter, thereby reducing the heat loss per unit mass of the gas mixture. The problem of heat transfer to the burner tube is of considerable interest in connection with current theoretical calculations of eigen-values in laminar flame propagation.

- (3) By comparison with other methods it has been established that Stevens' tangent method is more reliable than the direct area integration method. The limitations of this last conclusion will be discussed in Section I-C.
- (4) Experimental errors are generally minimized by making observation on gas mixtures with large burning velocities.
- (5) An appreciable redistribution of velocities in the stream takes place as the stream leaves the burner port. This edge effect results in an acceleration near the boundaries, in a deceleration near the axis, and affects the shape of the flame surface.

C. Selection of Method for Measuring Flame Velocity on Burner Tubes

In the present investigation the tangent method of Stevens was selected for the determination of laminar burning velocity. This selection is justified, to some extent, by the experiences of other investigators reviewed in Section I-B. Additional considerations supporting this choice are summarized briefly in the following paragraphs.

It is obviously desirable to have a close correlation between the conditions under which the actual burning velocity determination is made and the statements involved in the definition of the fundamental flame speed. The assumptions, or conditions, of the definition of U_b are: (a) all partial derivatives with respect to time are zero; (b) the temperature is constant across the surface T_1 of Fig. 1; (c) the normal component of velocity is constant across the surfaces dA_1 and dA_2 ; and (d) the surfaces bounding the stream tube are known.

If the flame is steady and the temperature of the burner tube

is constant with time, then the condition of steady state is met by any burner tube method.

Any surface in a burner flame which may be defined by optical or photographic means, such as the surface corresponding to the onset of luminosity, is, unfortunately, not at constant temperature. Gilbert⁽¹⁰⁾ has made temperature measurements throughout the flame front for laminar flames burning at reduced pressures. He found that the maximum temperature, T_{\max} , varies with the distance from the axis, r , as shown qualitatively in Fig. 3. Thus the chemistry of the reaction occurring at radius r_a is undoubtedly different from that at radius r_b . It is noted, however, that the temperature is nearly constant between the radii r_1 and r_2 . However, the values of r_1/R and r_2/R vary with the composition, the flow velocity, the burner size and the initial temperature of the gases.

The velocity profile across a cylindrical tube, such as a burner tube, in which there is a fully developed laminar flow of a fluid, is the familiar Poiseuille profile (Cf. Fig. 4). Thus in the actual burner tube the surface dA_1 meets the requirements of constant normal flow velocity only if an infinitesimal stream tube of radius r and thickness dr is considered as the stream tube 1 of the definition (Cf. Fig. 1). It should be pointed out that the average velocity exists at $r = 0.707R$.

The velocity profile across the burning surface, T_1 , is not easily determined. The flow direction at this surface depends principally upon the divergence of the gas stream from the burner port to the T_1 surface. With no flame front present the flow speeds up on the outside and slows down near the center of the stream after leaving the port, because of viscous effects. With the flame present, the only way to determine

the flow field is to place small particles, which will not disintegrate upon approaching or passing through the flame front, into the combustible mixture and to photograph their paths. With proper inertia corrections the flow field may be reasonably well determined by this method. However, if the flow rate is high and the lower extremity of the burning surface lies close to the port, as will be true of a fast burning or "strong" mixture, then the streamlines from the port to the T_1 surface may be approximated by lines parallel to the axis of the cone.

Selection of the T_1 surface of Fig. 1 is difficult. One might argue that the T_1 surface should be selected to coincide with the region of maximum rate of change of temperature with distance along a streamline. Schlieren photographs, shadow photographs, and temperature probes have shown that the maximum temperature gradient in a flame normally occurs upstream of the region which corresponds to the onset of luminosity and that the distance between the surface of onset of luminosity and the surface of maximum temperature gradient varies with burner size, mixture composition, initial temperature, and flow velocity.⁽¹⁰⁾⁽¹¹⁾⁽¹²⁾⁽¹³⁾

With the foregoing facts in mind, the relative merit of the two techniques, i. e., of the area integration method and of the tangent method, can be judged for the geometry of the particular flames under study.

In the tangent method the stream tube considered is the hollow cylindrical element of radius $0.707R$ and thickness dr bounded upstream by the burner port and downstream by the surface corresponding to the onset of luminosity. The accuracy of this method depends upon how

closely the following assumptions apply to the flame studied. (1) The divergence of this stream tube from the axial direction between the port and the burning surface is negligible, therefore dA_2 lies directly above dA_1 in Fig. 4. (2) The nature of the flame reactions between r_1 and r_2 of Fig. 3 is nearly constant and is representative of the reaction under study. (3) The radius of the stream tube considered, $0.707R$, lies between r_1 and r_2 of Fig. 3. (4) The flow is laminar, and therefore the velocity at r equals $0.707R$ is the average velocity passing through the burner port. The convenience of this selection of a representative radius for the elemental stream tube of the definition is shown by the relations developed in Fig. 2. (5) The surface dA_2 is parallel to the region defined by the onset of luminosity, but not necessarily coincident with it.

In the area integration method the stream tube considered is the entire stream of combustible mixture bounded upstream by the burner port and downstream by the surface dA_2 . The accuracy of this method depends upon how closely the following assumptions are met in the flame studied. (1) The leakage of gas around the port, i. e., the portion of gas remaining unburned, is negligibly small. (2) The flame reactions under study can be approximated by averaging over the entire flame surface. (3) In the absence of better information concerning the locus of points corresponding to the maximum rate of change of temperature along the streamlines, the onset of luminosity defines the surface dA_2 .

If it is assumed that the flow field is known, i. e., that the velocity pattern is accurately determined from the port through the flame

front, then application of the tangent method at various radii should yield results which would vary with radius, but which should be very nearly constant from $r = r_1$ to $r = r_2$.

On the other hand, employing the area integration method, if it is assumed that the leakage of gas around the port is negligibly small and the surface of maximum rate of change of temperature along the streamlines is accurately determined, the investigator must still accept the error introduced by assumption (2) of the area integration method. This error will obviously increase with increased heat transfer to the walls of the burner.

It was not possible to take schlieren photographs of each flame studied during the present investigations. It was equally impractical to determine the flow field between the burner port and the flame in each case.

Proponents of the area integration method have argued that only a small error is made if the surface defined by the onset of luminosity is selected in all cases. However, as the cone becomes steeper, this last statement is no longer true, and a slight error in selecting this surface will produce large variations in the area dA_2 of Fig. 2, causing large variations in the measured value of U_b . Obviously, the smaller the h/r ratio of the cone and the flatter the velocity profile, the better the method, approaching in the limit the Powling Flat Flame Method (Cf. Section I-D).

Exactly the reverse is true of the tangent method because the greater the height to radius ratio of the cone and the greater the flow velocity the smaller the divergence of the gas stream upon leaving the burner port.

In the flames studied in this work it was found that, if the height to radius ratio was greater than 8.0, the appearance, thickness, and slope of the reaction zone was constant between $r = 0.2R$ and $r = 0.85R$ in all but the hottest flames.

It is apparent from the foregoing discussion that in the practical case the tangent method will yield more reliable results than the area integration method when the cone observed is steep. For a flatter cone where the divergence of the stream from the axial direction is considerable and assumptions (1) and (3) of the tangent method break down together, the area method will be the better method.

At atmospheric pressure a mixture of oxygen and acetylene has a very high burning velocity, and the cones obtainable with burners of reasonable size are relatively steep; a representative value of the height to radius ratio is ten. This fact, plus a reluctance to accept the assumption that the representative flame reactions are better approximated by the average over the entire cross section than by the nearly constant reaction, as indicated by the small T_{\max} gradient, between r_1 and r_2 of Fig. 3, has made the tangent method more attractive for this work.

It can be argued that since the result desired is the effect of inert diluents upon the laminar flame velocity, the absolute value of the flame velocity without these diluents is rather unimportant. However, the per cent change in burning velocity due to the addition of an inert gas to the mixture depends upon this basic value, and for this reason, as well as for better correlation between the results obtained here and those obtained by other investigators using other methods of determining the burning velocity, it is reasonable to select the method which

seems to promise the more accurate value of the burning velocity under the conditions of the measurements.

D. Other Methods for Measuring the Laminar Burning Velocity

Reference has been made to methods for measuring U_b which are more elaborate than the burner tube method. Each of the methods has some limitations, but when the proper method is applied to a given system, the results obtained are generally more reliable than those determined by use of the burner method. Of these methods, three of the most widely used are: (1) the flat flame method; (2) the soap bubble or constant-pressure method; (3) the spherical bomb, or constant-volume method. These three methods will be described briefly in the following paragraphs.

(1) The Flat Flame Method

Powling⁽¹⁴⁾ developed the flat flame method in order to measure the burning velocity near the limits of inflammability where the value of U_b is extremely small. In the flat flame method a slow stream of a combustible mixture is passed through a large (e. g. 6 to 8 cm. diameter) vertically-mounted tube, and the gas velocity over the entire cross section of the burner port is rendered uniform by passing the mixture through a layer of small glass beads, a series of fine wire screens, and finally through numerous straight and narrow channels which terminate a short distance below the burner port (Cf. Fig. 5). A similarly adjusted stream of inert gas, such as nitrogen, is passed through a concentric tube surrounding the burner tube. By suitable adjustment of the flow of each stream it is possible to establish a very flat flame which remains suspended at some

distance above the port. In order to protect the flame against drafts caused by the entrance of the hot gases into the atmosphere, a wire screen is placed normal to the burner axis at some height above the combustion wave. Since it is difficult to stabilize this flat flame in any but very slow-burning mixtures, at least at atmospheric pressures, this method has a very limited application. The flame speed is calculated by dividing the gas flow by the area of the combustion wave.

(2) The Soap Bubble or Constant-Pressure Method

It has been noted that in each of the ordinary burner tube methods for measuring the burning velocity, the principal difficulty arises because the physical conditions are not uniform over the conical burning surface, thus forcing the investigator to rely upon some sort of averaging technique. He must either select a point at which he can reasonably assume that average conditions exist, as in the tangent method, or average the conditions over the entire flame surface, as in the area integration method. One obvious way to avoid this difficulty is to initiate the burning at the center of a sphere of combustible mixture and to allow the combustion wave to proceed outward in the form of an expanding spherical surface, as in a soap bubble at constant pressure. Under these conditions the velocity of the flame front in space is the sum of the speed with which the flame is progressing into the unburned mixture, U_b , and the speed with which the gases comprising the flame front are transported bodily due to the expansion behind the flame front. This expansion is caused by the heat liberated by the combustion processes and by any change in the number

of molecules per unit mass of the mixture as a result of the combustion processes. The soap bubble method was developed by Stevens⁽⁷⁾ in 1923. Refinements of the method have been proposed, notably by Fiock and Roeder⁽¹⁵⁾ in 1935.

The experimental procedure is quite straightforward. A soap bubble is blown from a container filled with the mixture to be studied over a pair of fine wire electrodes until the electrode gap is in the center of the bubble (Cf. Fig. 6). The mixture is then ignited by a spark and burns outward, the bubble expanding and keeping the pressure of the unburned charge ahead of the flame front at very nearly the pressure of the surrounding atmosphere. Observations are made until the bubble is broken and the mixture is completely burned.

For quantitative work the flame front is photographed through a horizontal slit which leaves only an image of the flame front diameter on the film (Cf. Fig. 6). The film is carried on a drum which rotates at a known speed around an axis parallel to the slit. A common method of obtaining the film speed is to put a time trace on the film (with a tuning fork) coincident with the size measurements. As the diameter of the burning sphere increases, a V-shaped trace is produced on the film. For most mixtures the sides of the V are found to be practically straight, showing that the flame front travels at nearly constant speed⁽¹⁶⁾. The speed of the flame front in space, S_g , can be calculated from the angle, α , at the vertex of the V, the known speed, F , of the film, and the magnification factor, m , of the camera. The basic relation is

$$S_g = mF \tan(\alpha/2) \quad (5)$$

Measurement on the film also permits the determination of the ratio of the volume of the burned products to the volume of the unburned charge, i. e., of the expansion ratio, E , for the mixture burning at constant pressure. If r is the radius of the bubble before firing, and R is the maximum radius of the sphere of hot gases as measured on the film, then

$$E = (mR)^3 / r^3 \quad (6)$$

Stevens⁽⁷⁾ showed that the burning velocity may be computed from the speed in space and the expansion ratio by use of the relation

$$U_b = S_s / E \quad (7)$$

Consider a steady flame front T_1 (Cf. Fig. 7) into which is flowing a combustible mixture at velocity U_b . Then U_b is the velocity at which the flame would advance into the stationary combustible mixture. Let S_s be the rate at which the products of combustion leave the flame, and let ρ and ρ' represent their corresponding densities; then

$$\rho U_b = \rho' S_s \quad (8)$$

and

$$\rho \frac{4}{3} \pi r^3 = \rho' \frac{4}{3} \pi R^3 \quad (9)$$

where r and R represent the initial and final radii of the gaseous spheres.

$$\therefore \frac{\rho'}{\rho} = \frac{r^3}{R^3} = \frac{U_b}{S_s} \quad (10)$$

or

$$U_b = S_s \frac{r^3}{R^3} = \frac{S_s}{E} \quad (11)$$

and since $S_g = R/t$, where t is the time of the reaction,

$$U_b = \frac{r^3}{R^2 t} \quad (12)$$

This soap bubble method can be used over a rather wide range of burning velocities, but it is subject to four practical limitations. First, it is often rather difficult to determine the final radius, R , of the sphere of hot gases. Second, if the mixture burns rapidly, i.e. is a "strong" mixture, the pressure wave from the flame front may be strong enough to break the bubble prematurely. Third, if the burning is slow enough, the bubble will rise during observation because of the buoyancy of the expanding gases inside. Corrections for this effect are not difficult to carry out. Fourth, if the solution from which the bubble is blown contains water, then the diffusion of water vapor to or from the bubble between the bubble and the gas and between the bubble and the surrounding atmosphere, makes it very difficult to know with precision the water vapor content of the mixture at the time of burning, unless the vapor pressure of water is initially the same in the soap solution, the combustible mixture, and the surrounding atmosphere. Thus unless a "dry" bubble solution can be obtained, this method cannot be used for determining the burning velocity of mixtures such as carbon monoxide-oxygen where the burning velocity is strongly dependent upon the water vapor content.

(3) The Spherical Bomb or Constant-Volume Method

Substitution of a spherical metal shell, or bomb, for the soap bubble makes it possible to vary the water vapor content of the mixture and the initial pressure.

When a centrally located spark occurs in a bomb filled with combustible mixture, a spherical flame is initiated and spreads in a manner similar to a constant-pressure wave. However, the walls of the bomb resist the outward flow of the gas produced by the expansion, and the unburned charge is compressed instead of merely being moved away by the advancing flame front. As a result of the steadily decreasing outward gas velocity, the flame front travels more slowly in space as it approaches the walls, whereas it may be propagating into the compressed and heated unburned charge at an ever increasing rate, i. e. U_b getting larger and larger. Interpretation of the data with proper allowance for the pressure rise in the bomb requires measurement, as a function of time, of the pressure, the expansion ratio and spacial velocity. With even the most sensitive pressure-recording instruments there is a small time lag between ignition and the recording of the first increment of pressure change. Non-adiabatic conditions exist near the end of burning because of heat transfer to the walls of the bomb. For these reasons both the instrumentation and the calculations which are required in order to interpret constant-volume data are considerably more complicated than for results obtained by the constant-pressure method. The slit, camera, rotating film, and time trace are employed much as in the soap bubble method.

Although the spherical bomb method does not have the simplicity of the soap bubble method, the variety of conditions under which it can be used and the wealth of data which can be obtained from one carefully executed experiment, have made it a useful method for flame speed measurements.

II. APPARATUS AND EXPERIMENTAL TECHNIQUE

The apparatus constructed for burning velocity determinations is shown schematically in Fig. 8. The gases were supplied to the system from standard commercial high-pressure tanks (T). The downstream pressure gauges (P), which were attached to the pressure regulator valves (R), were sensitive to about 1/10 psig.

Each gas was metered through Fischer & Porter heavy wall precision bore metering tubes using ball-type floats (F). These instruments usually deliver about $\pm 2\%$ of their calibrated flow, except near the limits of their respective operating ranges.

The volume flow of each gas was adjusted by the needle valves (N) placed just downstream of the flowraters in each line. The sensitivity of these valves in controlling the flow was quite satisfactory.

The mixing chamber (M) also served as an effective flashback arrestor and consisted of a cast iron pipe about 3.5 inches in diameter and 24 inches long, capped at each end and filled with several thousand small tubular glass beads. The inlet lines were tapped into the pipe 60° apart at the upstream end of the chamber. The outlet was tapped into the cap at the downstream end of the chamber. Since the observed flames were steady, it was concluded that good mixing was accomplished in the mixing chamber.

The burner (B) used for the present studies was a high quality oxygen-acetylene torch tip. Its inside diameter (cold) was 0.070 ± 0.002 inches and was determined by inserting drill cylinders of known diameter until a snug fit was obtained.

By means of a double-convex lens (L) the image of the flame

cone (C) was magnified and projected onto tracing paper (TP). A plane mirror (PM) served to place the image on a horizontal surface for convenience in tracing the outline of the image formed. The tracing paper was held in place on the clear glass (G) by spring steel clamps. Magnifications used were from 12:1 to 15:1. The system was aligned until a sharp and true image was observed on the tracing paper. A satisfactory tracing material was a translucent plastic plate which was found to transmit enough light at the magnifications used with the cooler flames and still give a sufficiently clear image on the upper surface to define the various regions of the inner cone. It is estimated that errors in optical alignment could not contribute an error of more than 1% to the measured value of the burning velocity.

Copper tubing was used throughout, except for the lines from the pressure regulators to the flowraters and for the last two feet of the line from the mixing chamber to the burner, where rubber hose was used.

Figure 9 shows a typical image (I) of the inner cone of the flame as formed on the tracing paper and the tangents (T_1 and T_2) which were drawn on the paper parallel to the upstream side of the bright image. In each measurement an attempt was made to adjust the flow velocity to such a value that the slope of the line corresponding to onset of luminosity would be constant from about $0.2R'$ to $0.85R'$, where R' represents the magnified radius of the burner port. With all but the hottest flames this was achieved with an h/r ratio of between 8 and 12, where h represents the height of the triangle traced on the paper and r represents the half-base of this triangle. Successive measurements on the

same flame showed a reproducibility of about two percent in the measured burning velocity, U_b . Larger errors were observed if an attempt was made to reproduce experimental results on different days.

The experiences of other investigators have indicated that competent people establish limits of accuracy for certain systems only to find that their results vary from data obtained with similar systems and limits of accuracy by margins far outside of the predicted limits of accuracy. On the basis of this well-known fact, it is to be expected that absolute estimates for the laminar burning velocity are less significant than systematic studies of the variation of burning velocity with composition. For this reason the data were taken in consecutive "runs" in which the fuel to oxygen ratio was held fixed and the inert gas composition was varied. The total duration of a "run" was about one hour, and during this time adjustments of all parts of the system were held to a minimum. The temperature of the room in which the determinations were made was at all times between 70°F and 72°F.

III. EXPERIMENTAL RESULTS AND DISCUSSION

The results of the experimental work are presented in graphical form in Figs. 10 through 16. In Figs. 10, 11, and 12 the laminar burning velocity in feet per second is plotted against the percentage by volume of inert gas added to the mixture. In Fig. 10 are shown the lean compositions with a molar fuel to oxygen ratio of 0.2, i. e., one half stoichiometric. Similar data for the stoichiometric mixture, ($f = 0.4$) and for rich mixture ($f = 0.8$) are shown in Figs. 11 and 12, respectively. Figures 13 through 16 are cross-plots containing the same experimental data for argon, carbon dioxide, helium, and nitrogen, respectively, with data for all three mixture ratios appearing on one plot. The data shown in Figs. 10 to 16 can be accounted for qualitatively by utilizing a thermal theory of laminar flame propagation.

For a fixed percentage of inert gas, the laminar burning velocity decreases most rapidly for CO_2 , less rapidly for N_2 and A, and least for He. These observations can be accounted for in terms of the well-known results obtained, for example, from Semenov's⁽¹⁷⁾ equation for a second order burning process, which leads to the conclusion that

$$U_b = \text{constant} \left[T_c / (T_c - T_o) \right] \lambda^{(1/2)} \left[a / (1 + a r \phi) \right]^{(1/2)} \left[1 - (0.9 / \phi) \right]^{(1/2)} \\ \times \exp(-E/2RT) \quad (13)*$$

*Note: This is the simplified form of Semenov's equation presented in the A. E. thesis of D. L. Ritter, California Institute of Technology, May 1953.

- where α = moles of oxygen divided by the sum of the moles of oxygen and the inert gas;
- ϕ = moles of fuel per mole of oxygen divided by r , i. e. $\phi = f/r$;
- r = moles of fuel per mole of oxygen for the stoichiometric mixture ratio, i. e., $r = 0.40$;
- T_c = adiabatic flame temperature;
- T_o = initial temperature of the mixture;
- λ = effective thermal conductivity, which should be evaluated at a temperature close to the adiabatic flame temperature;
- E = effective activation energy for the flame reactions;
- R = molar gas constant

Equation (13) has been shown to apply for fixed initial temperatures and pressures. It is evident by reference to this equation that for fixed values of α and ϕ , corresponding to fixed values of f and of volume percent of inert gas, the laminar burning velocity varies as the square root of the thermal conductivity and as $\exp(-E/2RT_c)$. Since the molar heat capacities at constant pressure decrease in the order $C_p(\text{CO}_2) > C_p(\text{N}_2) > C_p(\text{He}) \doteq C_p(\text{A})$ it is clear that T_c will increase in the order $(T_c)\text{CO}_2 < (T_c)\text{N}_2 < (T_c)\text{He} \doteq (T_c)\text{A}$. Hence the factor $\exp(-E/2RT_c)$ decreases in the order

$$[\exp(-E/2RT_c)]_{\text{He,A}} > [\exp(-E/2RT_c)]_{\text{N}_2} > [\exp(-E/2RT_c)]_{\text{CO}_2}$$

The thermal conductivities for He, A, N_2 , and CO_2 decreases in the order

$$(\lambda)_{\text{He}} > (\lambda)_{\text{N}_2} > (\lambda)_{\text{A}} > (\lambda)_{\text{CO}_2}$$

with the thermal conductivity of He being much larger also than that of any of the combustion products or reactants, except H and H₂, which may be present in the flame. Hence it is not surprising to find

$$(U_b)_{CO_2} < (U_b)_{N_2} \doteq (U_b)_A < (U_b)_{He}$$

Judging from the available experimental data, the products of the coefficients

$$(\lambda)_A^{(1/2)} \left[\exp(-E/2RT_c) \right]_A \text{ and } (\lambda)_{N_2}^{(1/2)} \left[\exp(-E/2RT_c) \right]_{N_2}$$

must be nearly the same for A and N₂.

The initial increase in burning velocity for addition of He suggests that the increase in thermal conductivity produced by addition of He more than compensates for any decrease in T_c for fuel-rich and for fuel-lean mixtures (Cf. Figs. 10 and 12).

A more quantitative correlation of the experimental data with the theoretical relation given in Equation (13) does not appear to be warranted at the present time in view of the gross approximations made in the derivation of this relation. Furthermore, it is not entirely clear at what particular temperatures the value of λ is to be calculated in order to be useful for quantitative calculations based on Equation (13). In this connection it may be of interest to note that Wheatley and Linnett⁽¹⁸⁾ considered that diffusion of atoms and radicals back from the flame front had an important effect on U_b. Energy transport by diffusion has been neglected in the derivation of Equation (13). Wheatley and Linnett calculated thermal conductivities at room

temperature, which is at best a very poor approximation. Bartholome⁽¹⁹⁾ has pointed out that, for methane-oxygen flames, thermal theories of flame propagation give excellent agreement with the experimental data provided thermal conductivities at temperatures close to the adiabatic flame temperatures are used.

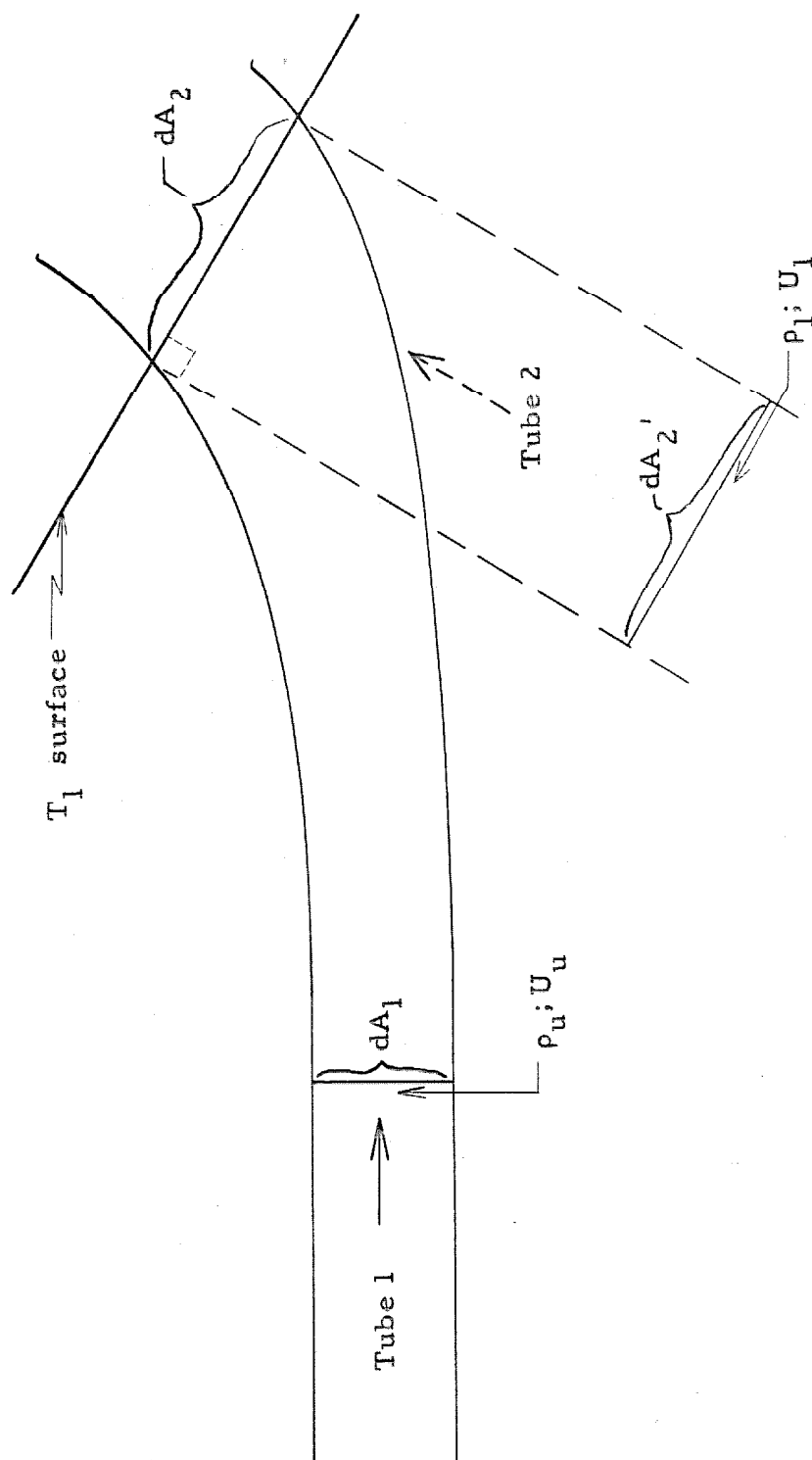
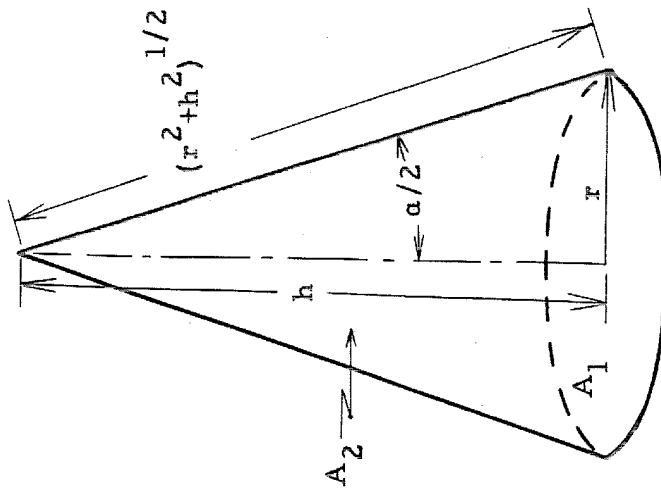


Fig. 1. Diagram showing the model of Lewis and von Elbe upon which the generally recognized definition of laminar flame velocity is based.



$A_1 \equiv$ Area of base of right circular cone
 $= \pi r^2$

$A_2 \equiv$ Slant area of right circular cone
 $= \pi r(r^2 + h^2)^{1/2}$

$$\begin{aligned} A_1/A_2 &\equiv \pi r^2 / \pi r(r^2 + h^2)^{1/2} = r/(r^2 + h^2)^{1/2} \\ &= \text{sine } (\alpha/2) \end{aligned}$$

Fig. 2. Diagram showing the relation between the half-angle of a conical flame and the ratio of the cross-sectional area of the burner tube to the surface area of the flame cone.

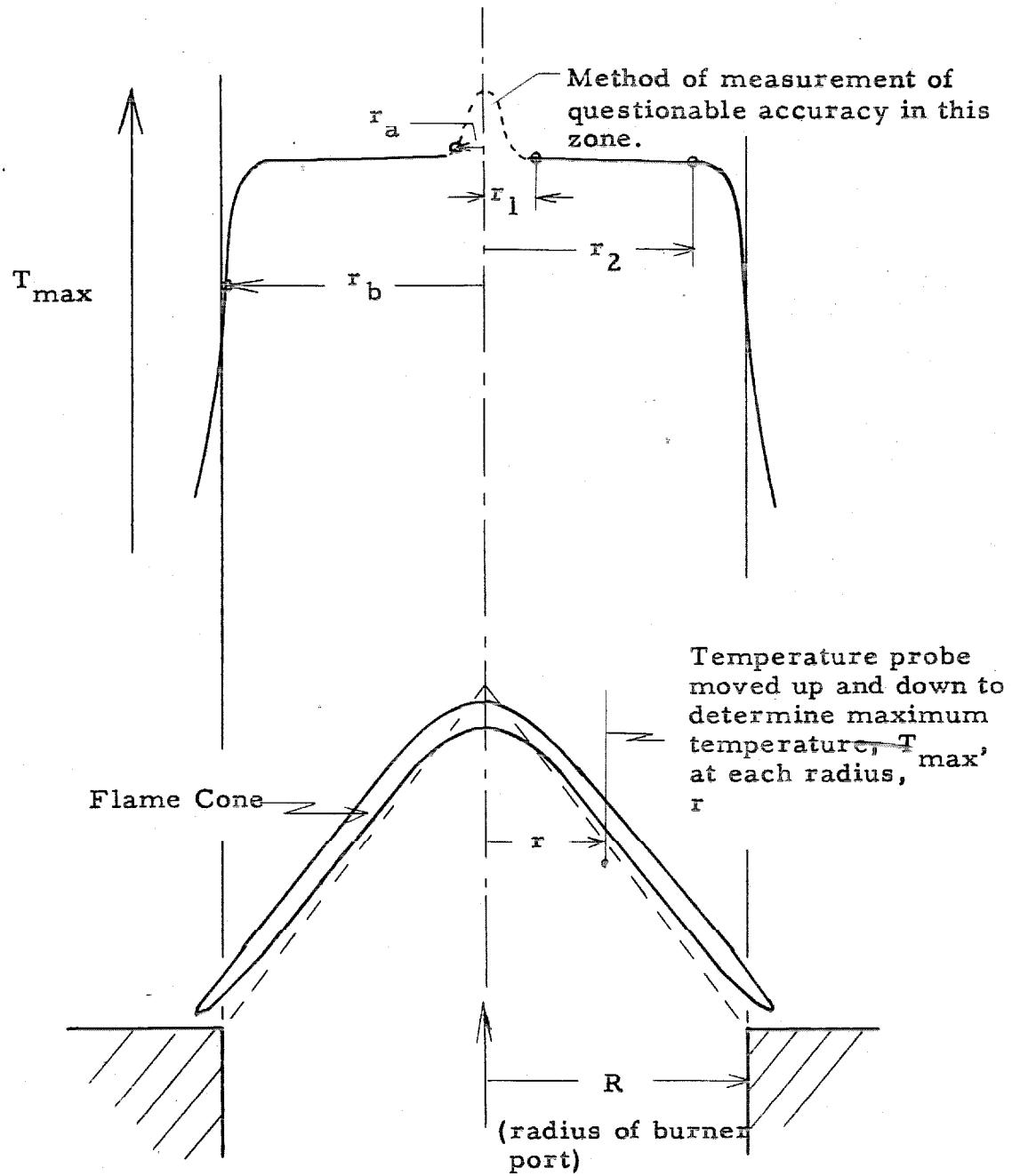


Fig. 3. Diagram showing qualitatively the relation between the maximum temperature (T_{\max}) observed in traversing a conical flame and the distance from the axis of the burner tube.

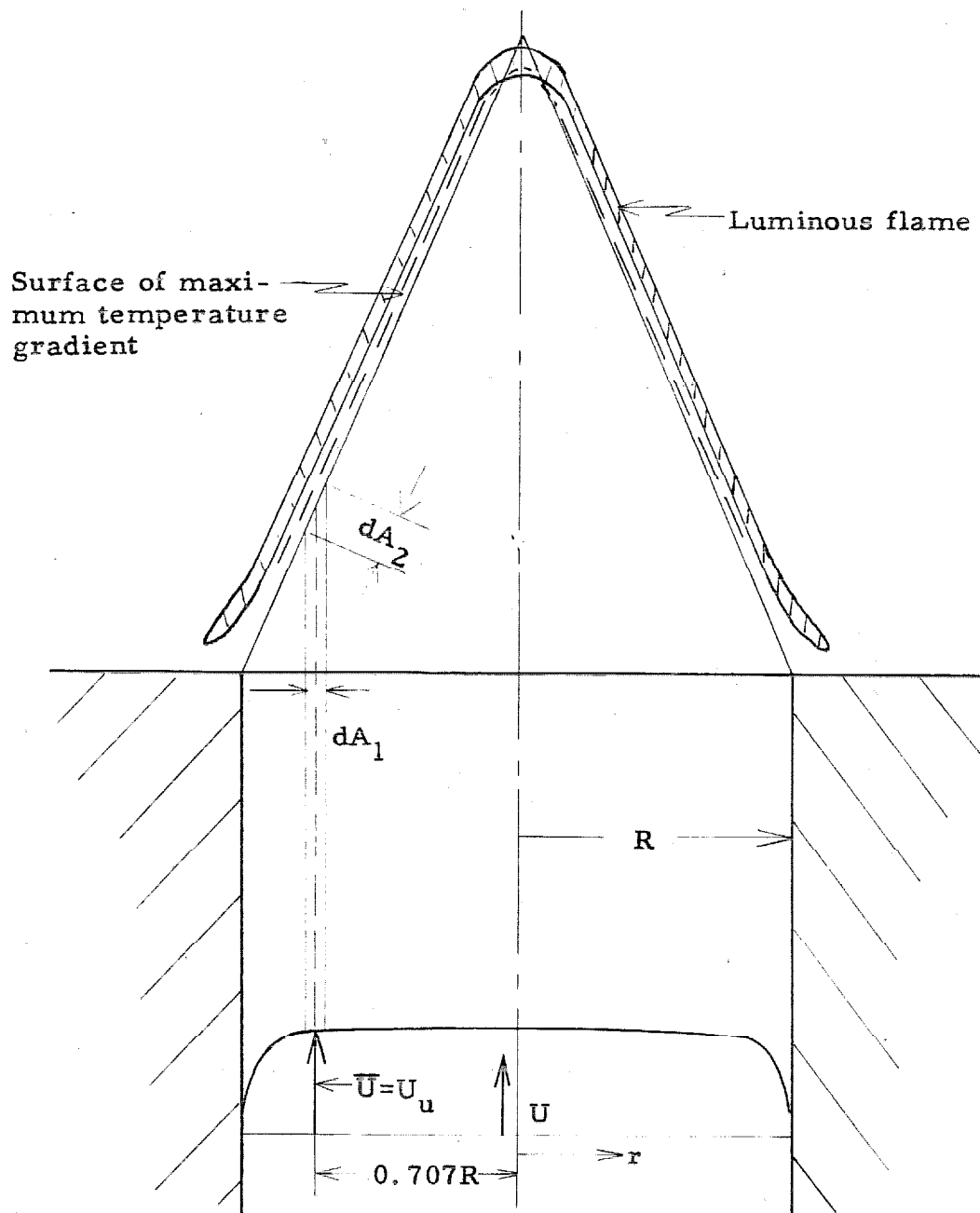


Fig. 4. Diagram showing a Poiseuille velocity profile in a burner tube and the stream tube considered in fitting the tangent method of measuring laminar burning velocity to the definition of laminar burning velocity.

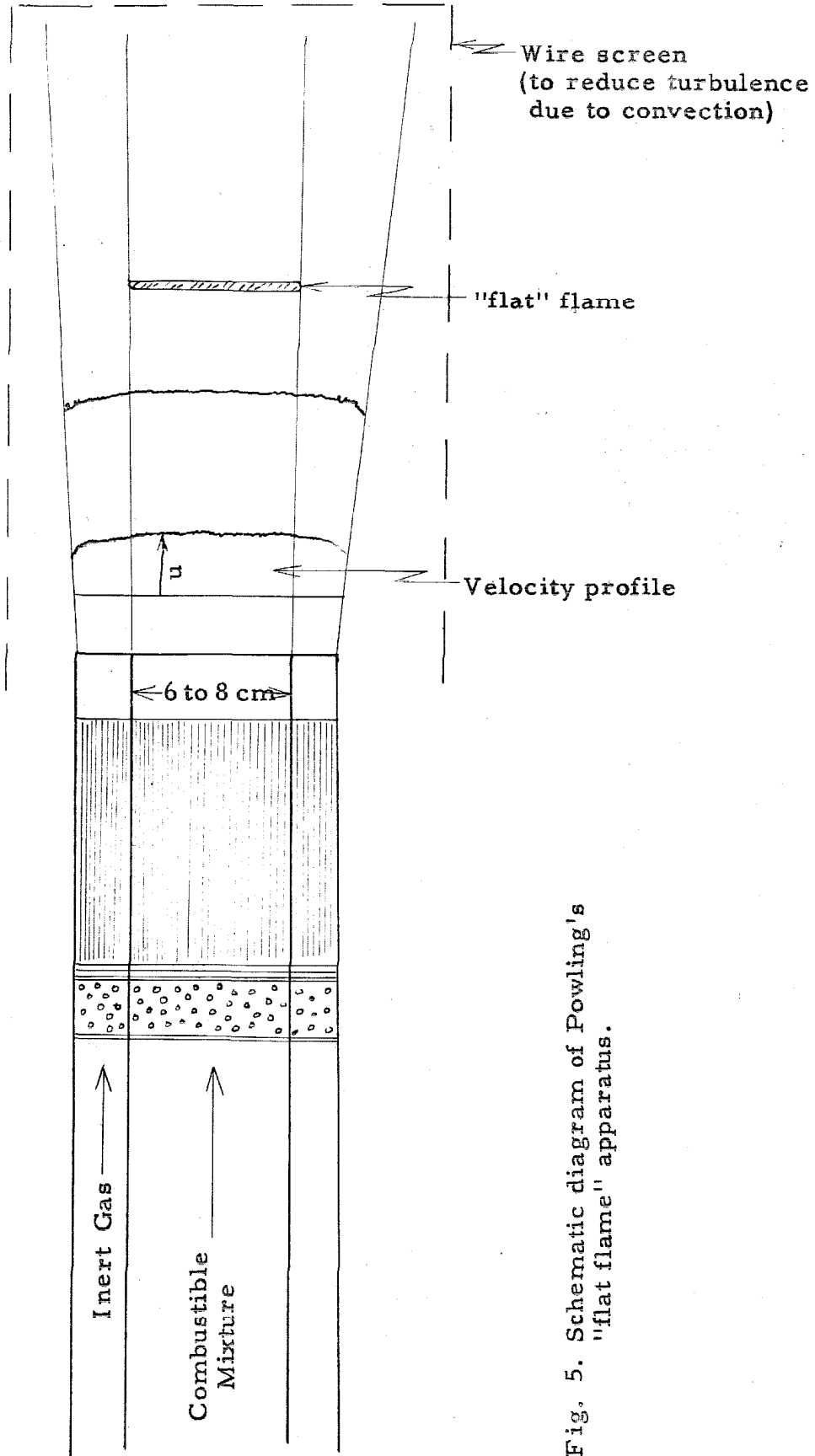


Fig. 5. Schematic diagram of Powling's "flat flame" apparatus.

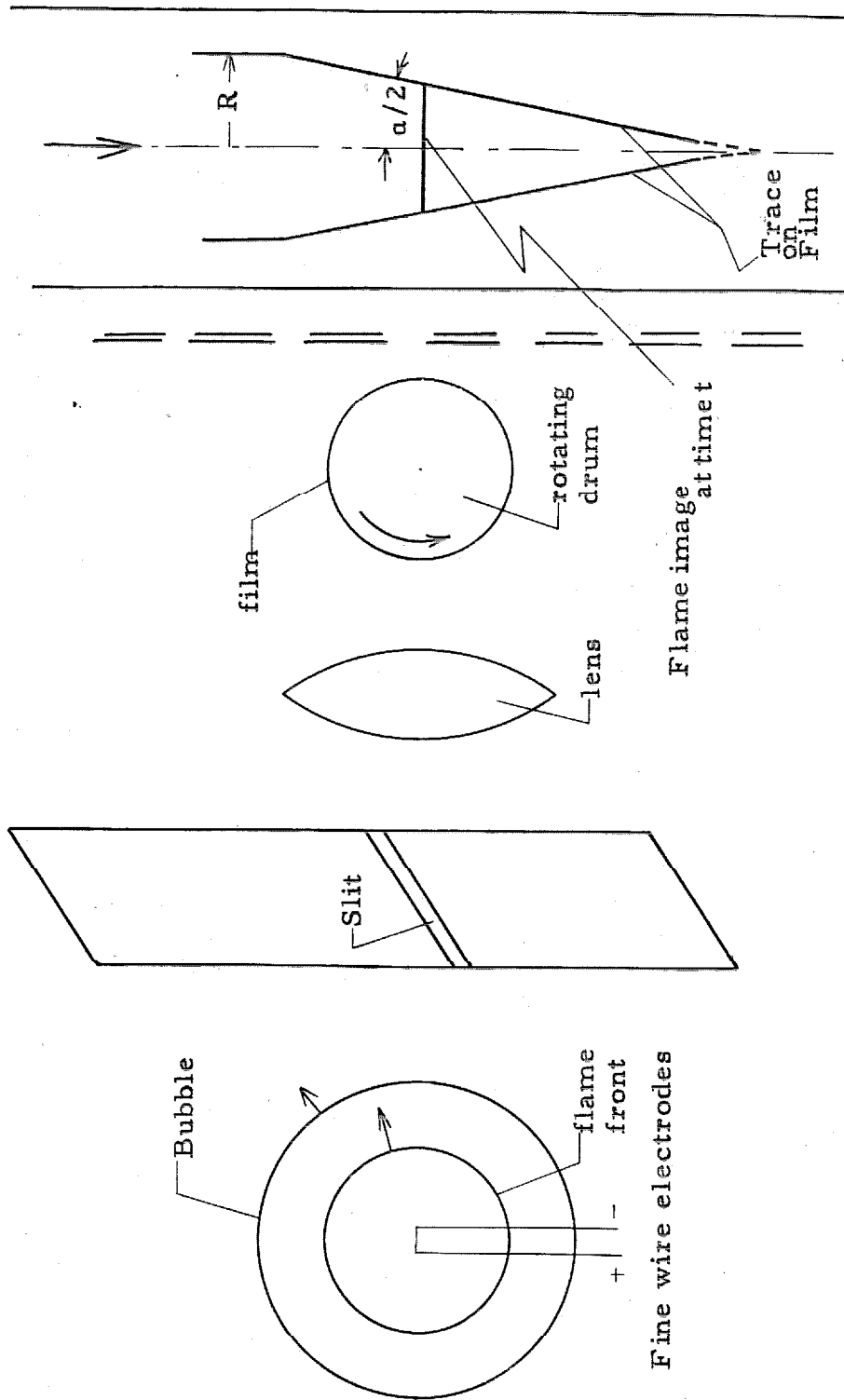


Fig. 6. Schematic diagram of an apparatus for determining burning velocities by the soap bubble method.

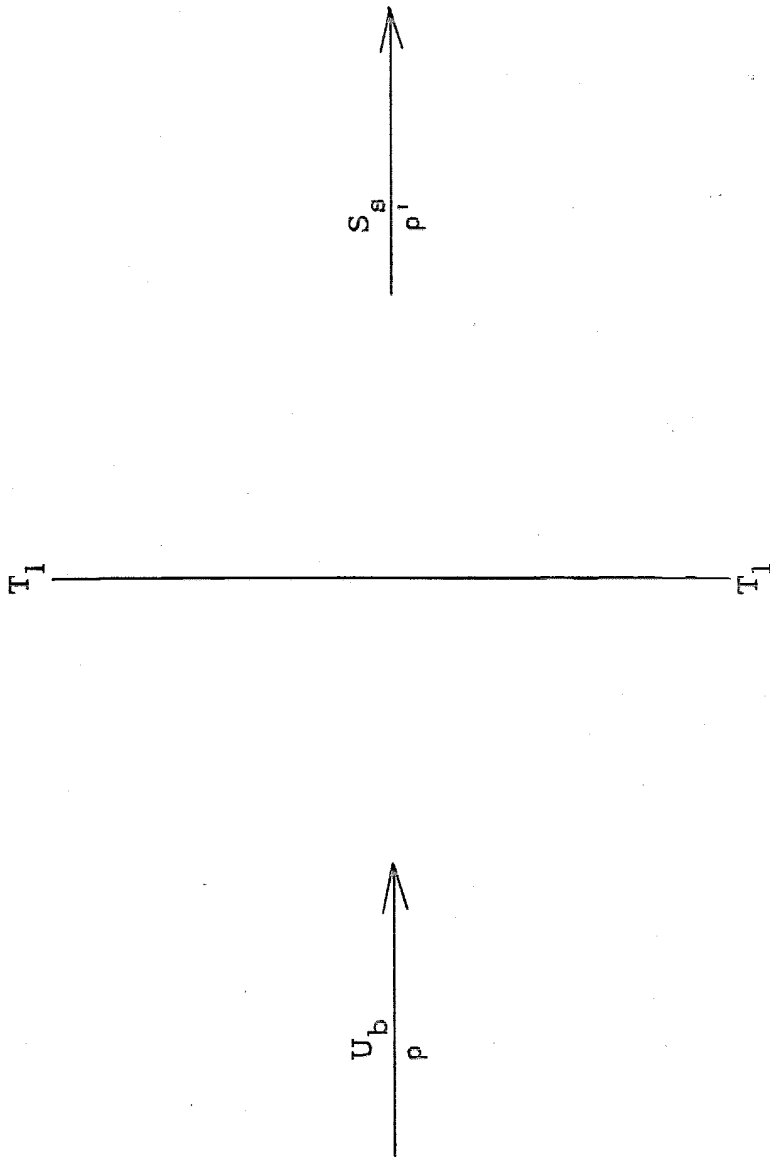


Fig. 7. Diagram showing the relation between the burning velocity, (U_b) , the speed in space of the combustion wave, (S_s) , and the expansion ratio, (E) , for the soap bubble method of determining the burning velocity.

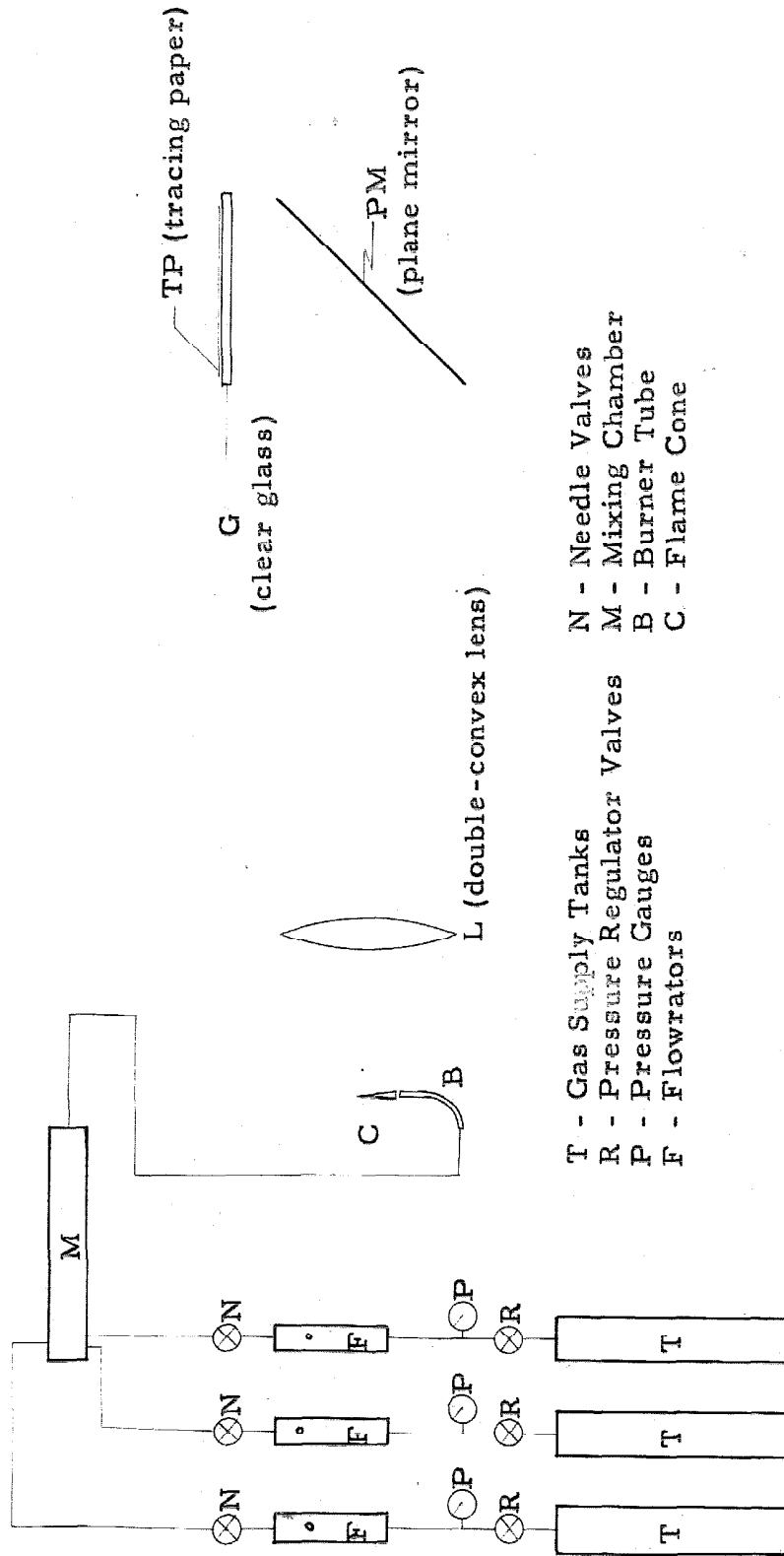


Fig. 8. Schematic diagram of the apparatus built and used to obtain the laminar burning velocity data presented in this thesis.

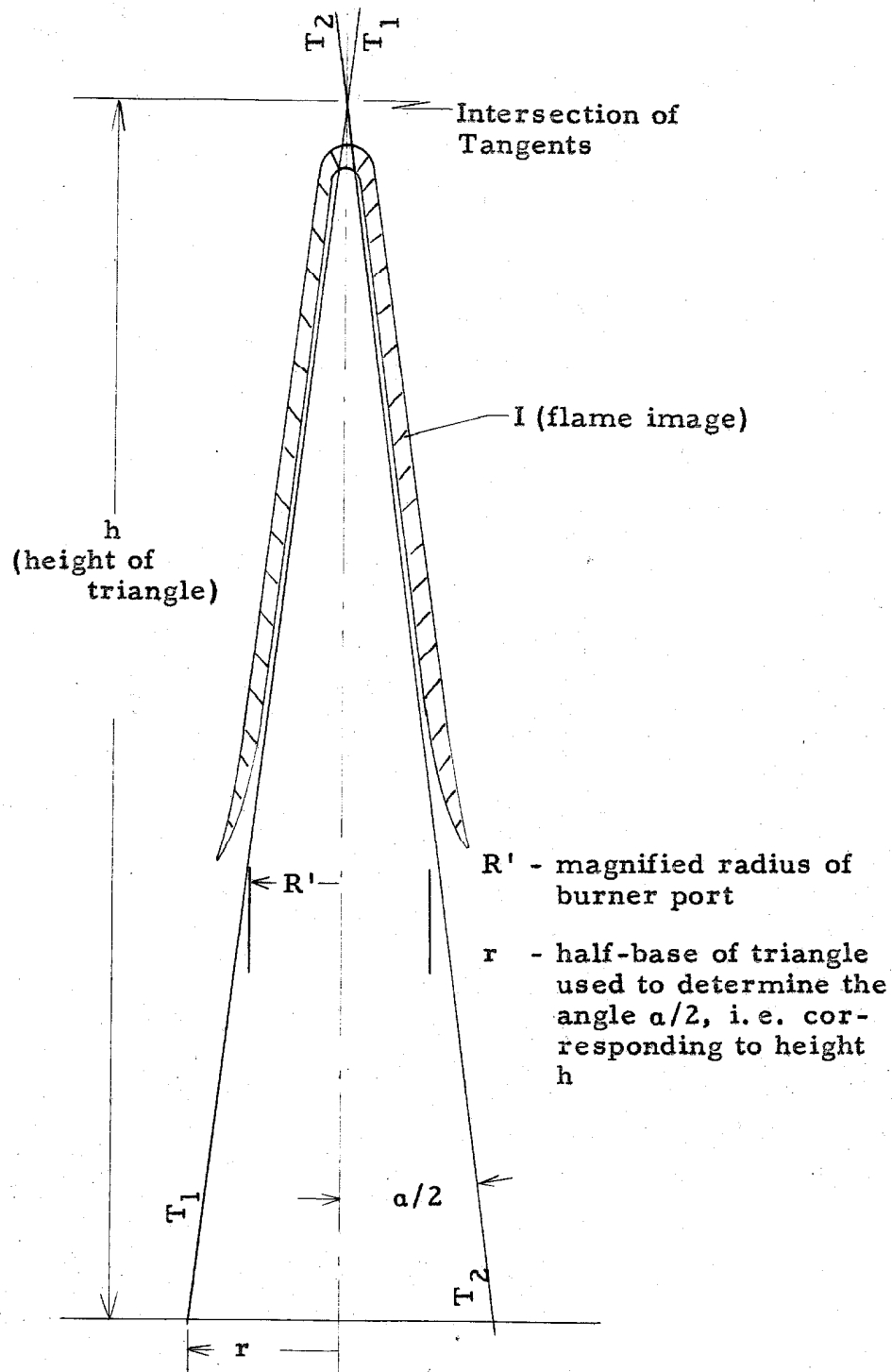


Fig. 9. Diagram showing a typical inner-cone image, actual size, as observed on the tracing paper and the experimental method of obtaining data from this image.

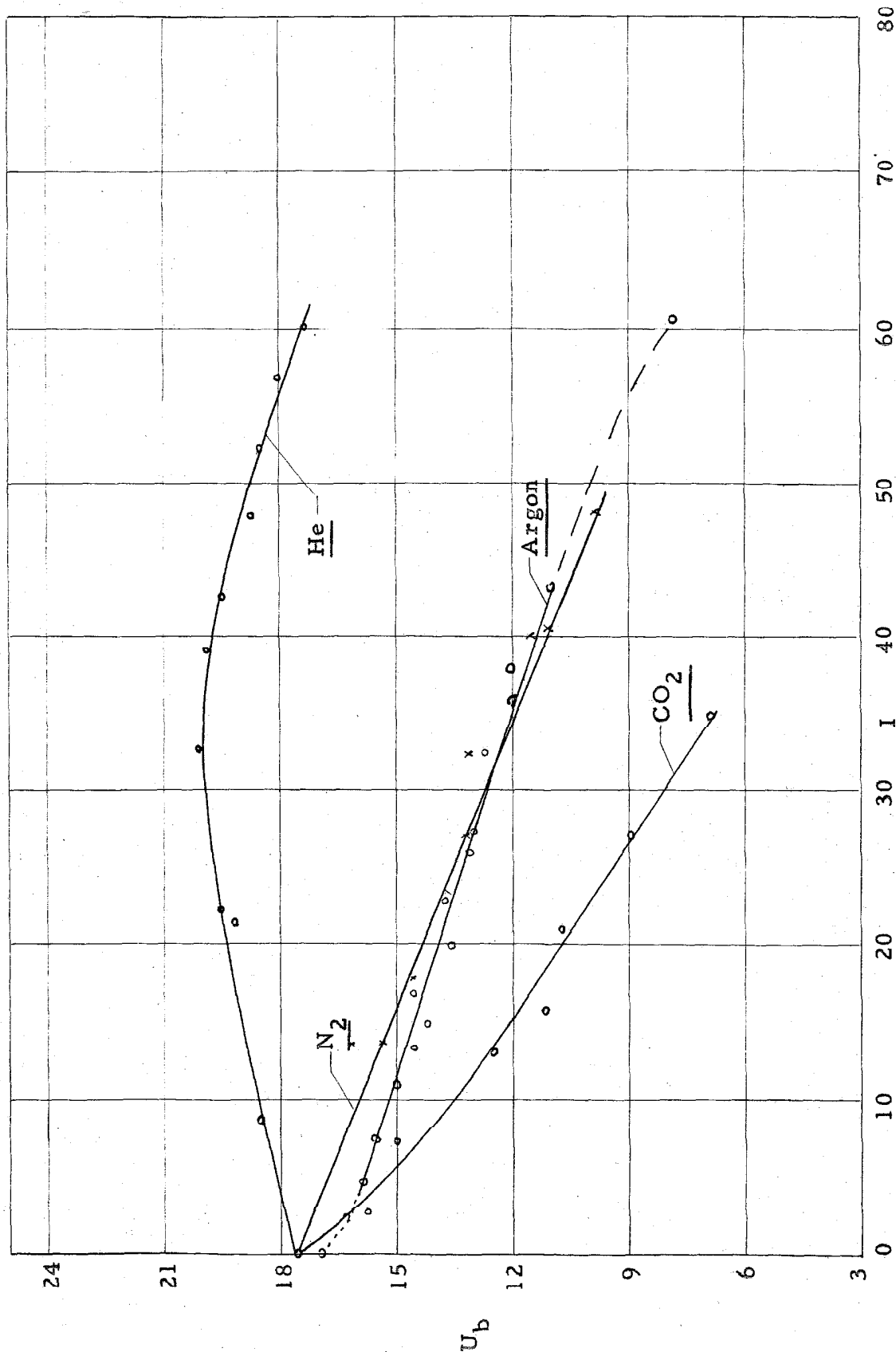


Fig. 10. Plot of laminar burning velocity in feet per second (U_b) versus volume percent of inert gas (I) for the inert gases Argon, Carbon Dioxide, Helium, and Nitrogen, where the molar ratio of acetylene to oxygen is constant for all mixtures and equal to 0.2, i.e., one-half the stoichiometric fuel/oxygen ratio.

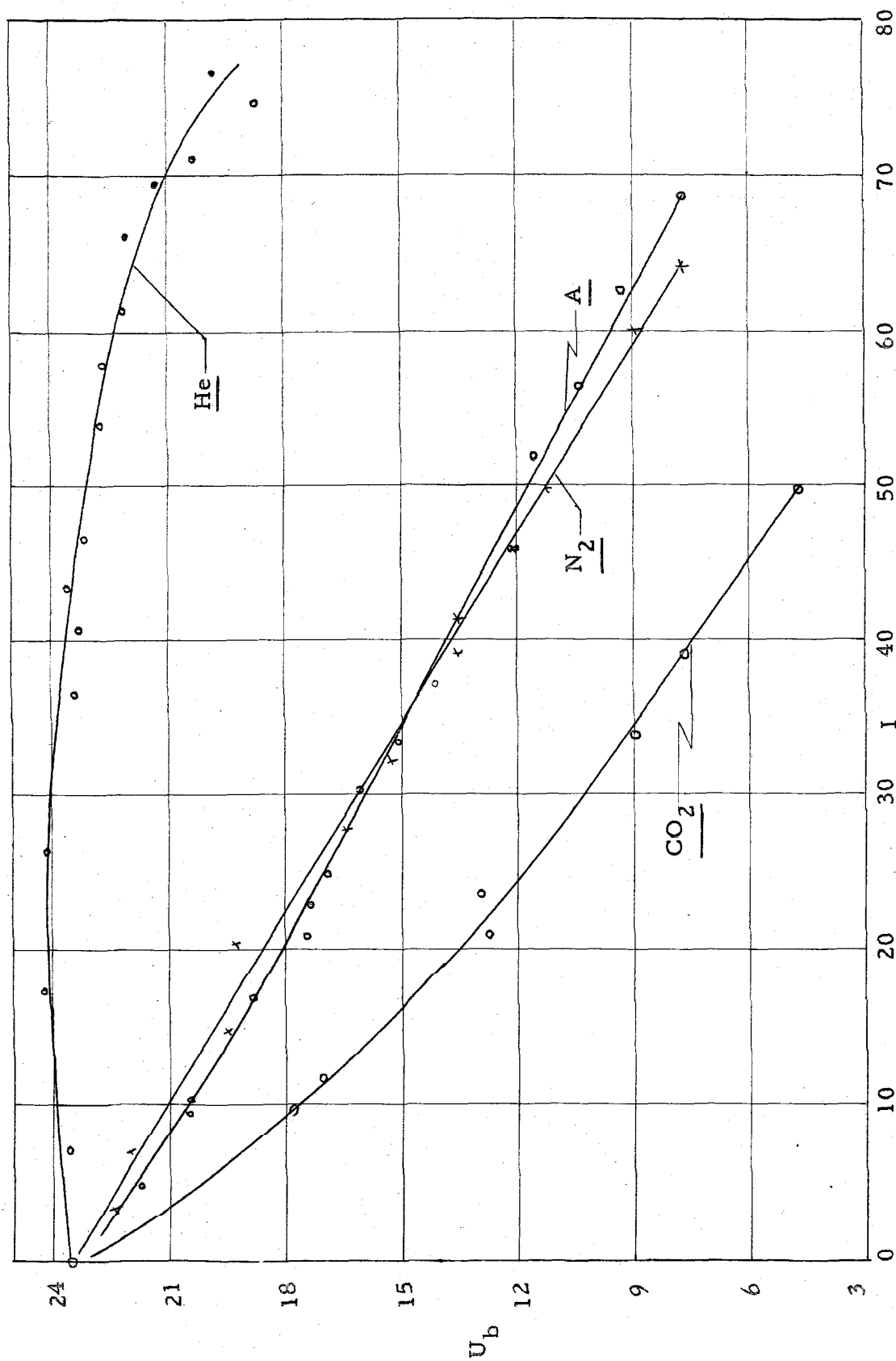


Fig. 11. Plot of laminar burning velocity in feet per second (U_b) versus volume percent of inert gas (I) for the inert gases Argon, Carbon Dioxide, Helium, and Nitrogen, where the molar ratio of acetylene to oxygen is constant for all mixtures and equal to 0.4, i. e., the stoichiometric fuel/oxygen ratio.

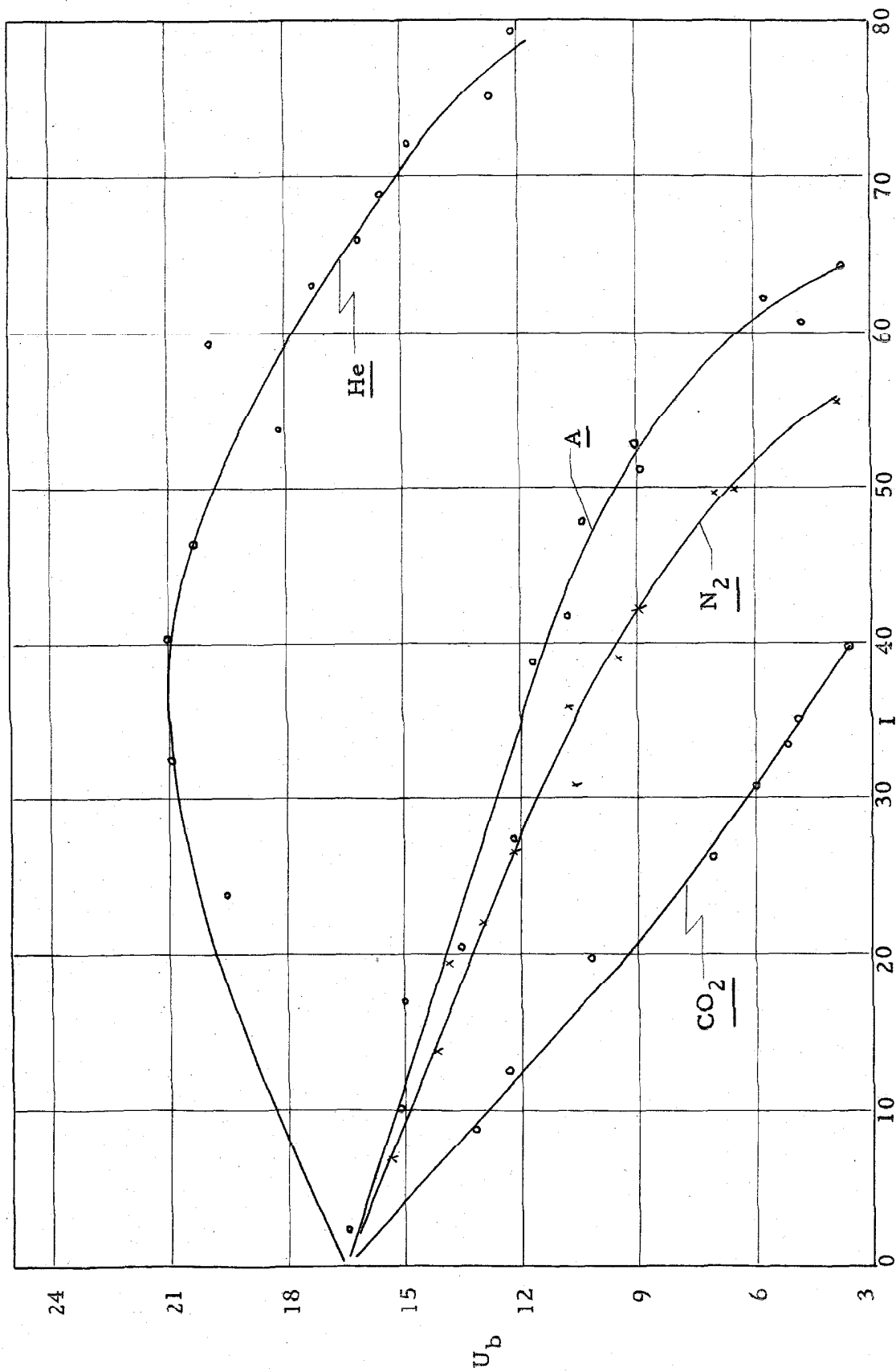


Fig. 12. Plot of laminar burning velocity in feet per second (U_b) versus volume percent of inert gas (I) for the inert gases Argon, Carbon Dioxide, Helium, and Nitrogen, where the molar ratio of acetylene to oxygen is 0.8, i. e., twice the stoichiometric fuel/oxygen ratio.

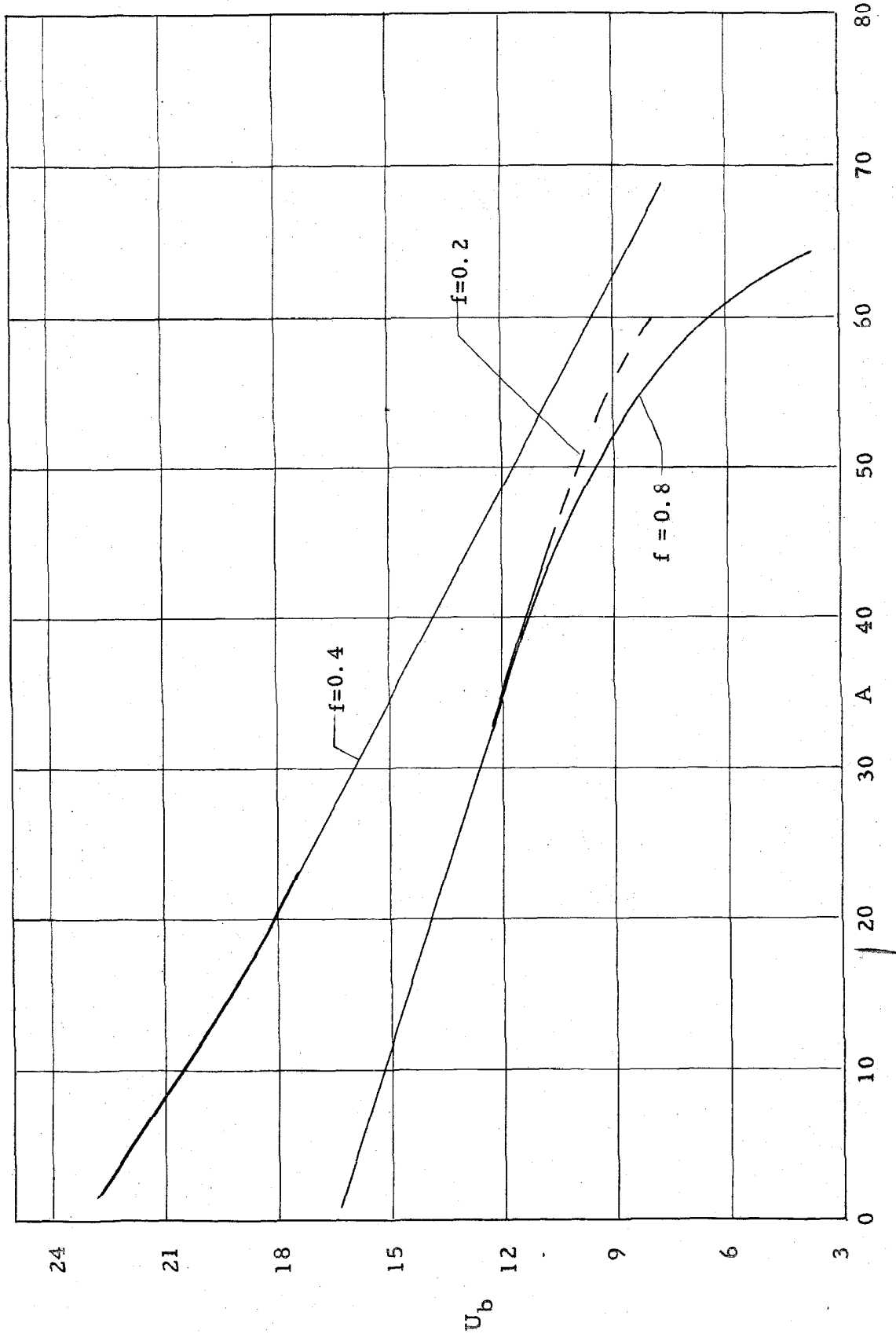


Fig. 13. Plot of laminar burning velocity in feet per second (U_b) versus volume percent of Argon (A) for the molar acetylene to oxygen ratios of 0.2, 0.4, and 0.8, i.e. one-half stoichiometric, stoichiometric, and twice stoichiometric fuel/oxygen ratios respectively.

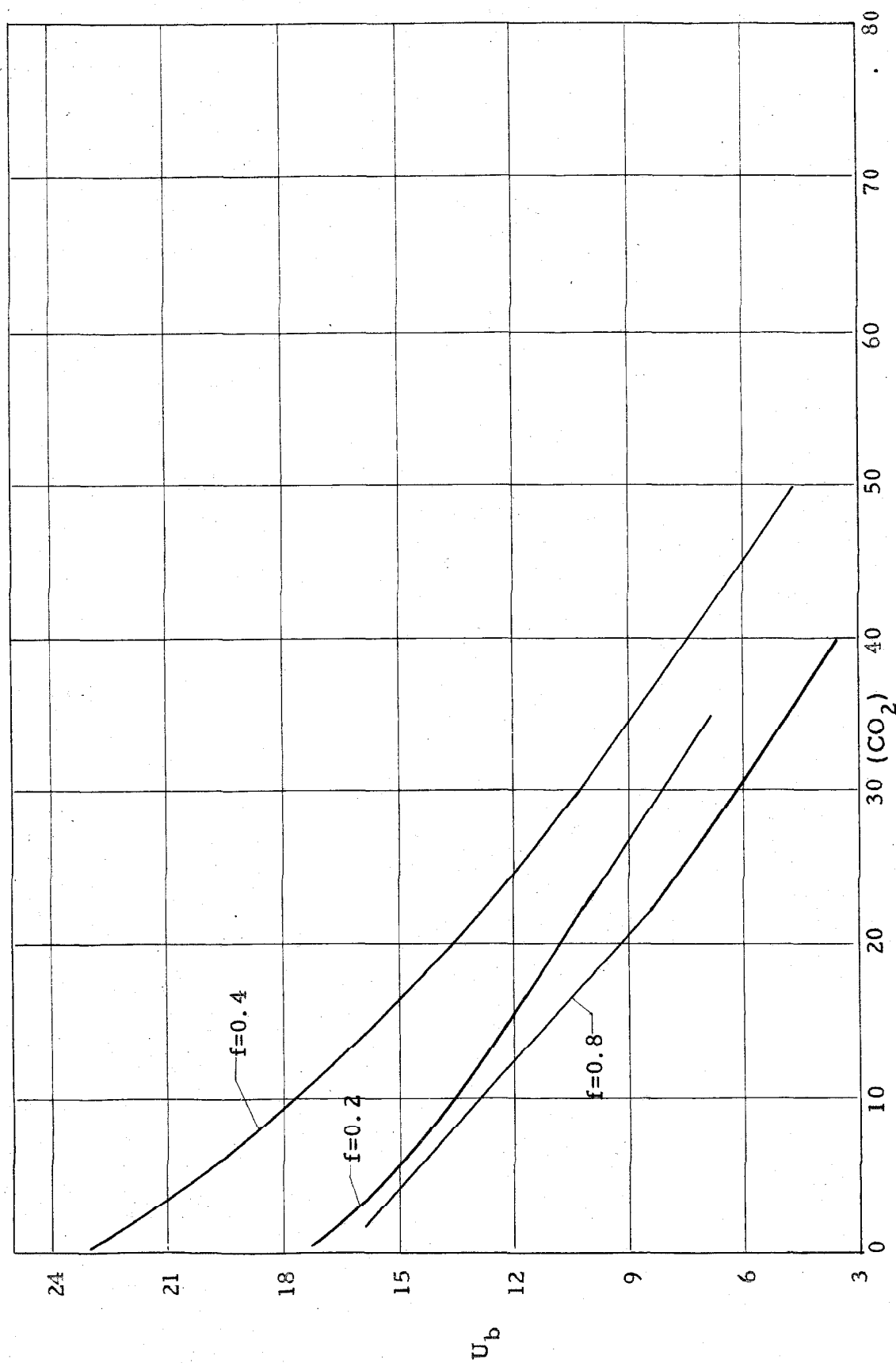


Fig. 14. Plot of laminar burning velocity in feet per second (U_b) versus volume percent of Carbon Dioxide (CO_2) for the molar acetylene to oxygen ratios of 0.2, 0.4, and 0.8, i.e., one-half stoichiometric, stoichiometric, and twice stoichiometric fuel/oxygen ratios respectively.

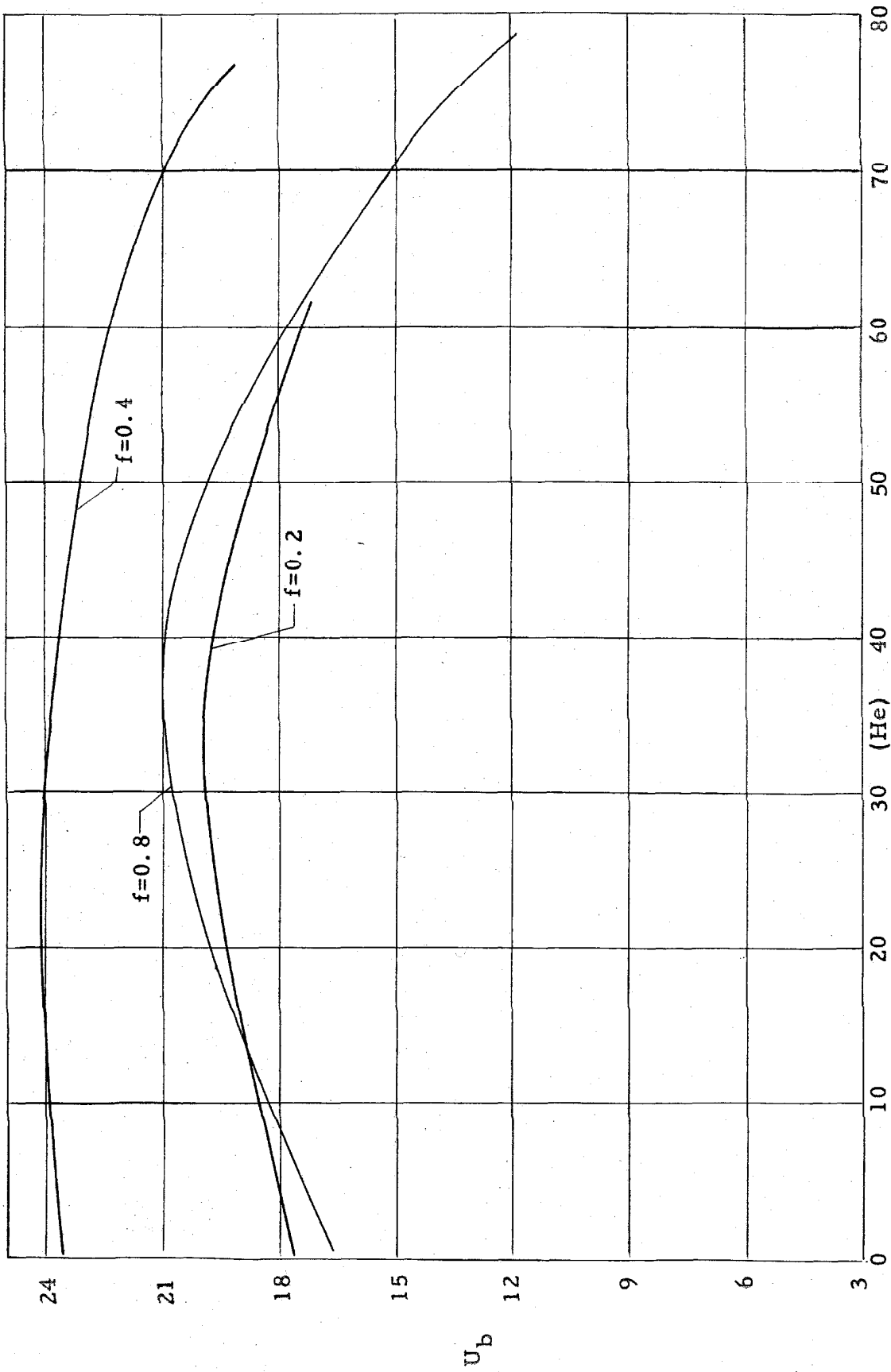


Fig. 15. Plot of laminar burning velocity in feet per second (U_b) versus volume percent of Helium (He) for the molar acetylene to oxygen ratios of 0.2, 0.4, and 0.8, i.e., one-half stoichiometric, stoichiometric, and twice stoichiometric fuel/oxygen ratios respectively.

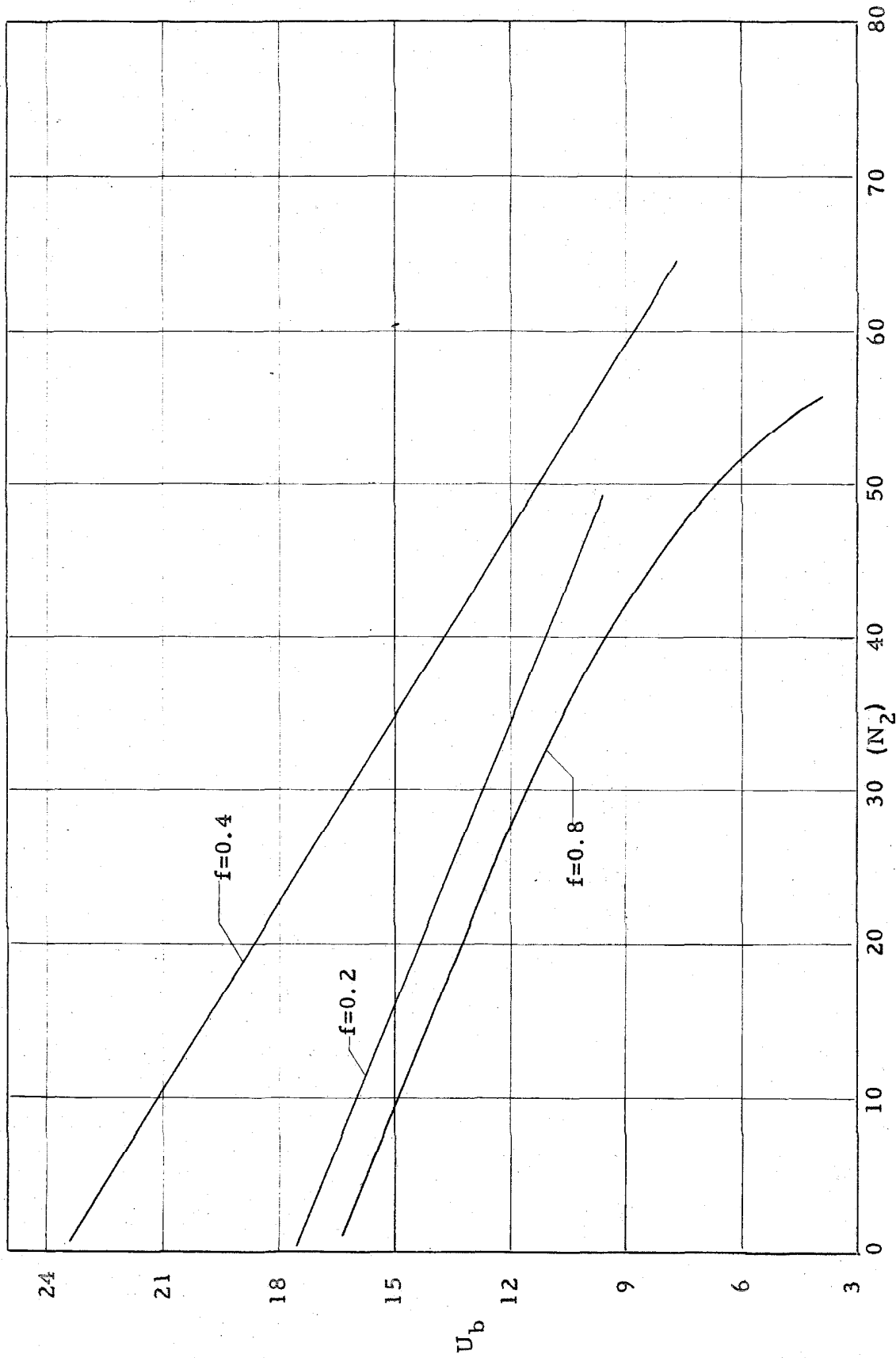


Fig. 16. Plot of laminar burning velocity in feet per second (U_b) versus volume percent of Nitrogen (N_2) for the molar acetylene to oxygen ratios of 0.2, 0.4, and 0.8, i.e., one-half stoichiometric, stoichiometric, and twice stoichiometric fuel/oxygen ratios respectively.

REFERENCES

1. B. Lewis and G. von Elbe, "Combustion, Flames and Explosions of Gases", Academic Press Inc., New York, 1951.
2. W. Jost, "Explosions und Verbrennungsvorgänge in Gasen", Springer, Berlin, 1939.
3. R. Bunsen, Poggendorffs Ann., 131, 161 (1866).
4. M. Gouy, Ann. chim. phys., 18, 27 (1897).
5. W. Michelson, Wiedemanns Ann. 37, (1889).
6. L. Ubbelohde and E. Koelliker, J. Gasbelencht, 59 19-57, (1916).
7. F. W. Stevens, NACA Tech. Repts., 176, 280, 305, 337, 372, (1923).
8. F. A. Smith and S. F. Pickering, J. Research Natl. Bur. Standards, 17, 7 (1936) RP 900.
9. F. A. Smith, Natl. Bur. Standards, U.S. Dept. of Commerce and Chem. Review 21, (1937).
10. M. Gilbert, "Investigation of Low Pressure Flames", JPL Rept. No. 4-54.
11. K. Wohl, Third Symposium on Combustion and Flame Explosion Phenomena, Williams and Wilkins Co., Baltimore, (1949).
12. J. J. Broeze, H. van Driehl and L. A. Peletier, Schriften deut. Akad. Luftfahrtforsch, (1939).
13. B. Thorley, R. Long, and F. H. Garner, Paper on a Comparison of Schlieren, Shadow, and Luminous Methods of

Determining Burning Velocities, Paper No. 92 in Abstracts of Papers, Fourth Symposium (International) on Combustion (1952).

14. J. Powling, Fuel 28, 25 (1949).
15. E. F. Fiock and C. H. Roeder, NACA Rept. Nos. 532 (1935) and 553 (1936).
16. E. F. Fiock and F. Marvin Jr., Chem. Reviews 21, (1932).
17. N. N. Semenov, NACA TM 1026, (1942).
18. P. J. Wheatley and J. W. Linnett, Trans. Faraday Soc., 48, 338 (1952).
19. E. Bartholome, Naturwissenschaften, 36, 171-175, 206-213, (1949).

LIST OF FIGURES

<u>Figure No.</u>		<u>Page No.</u>
1	Diagram showing the model of Lewis and von Elbe upon which the generally recognized definition of laminar flame velocity is based.	24
2	Diagram showing the relation between the half-angle of a conical flame and the ratio of the cross-sectional area of the burner tube to the surface area of the flame cone.	25
3	Diagram showing qualitatively the relation between the maximum temperature (T_{\max}) observed in traversing a conical flame and the distance from the axis of the burner tube.	26
4	Diagram showing a Poiseuille velocity profile in a burner tube and the stream tube considered in fitting the tangent method of measuring laminar burning velocity to the definition of laminar burning velocity.	27
5	Schematic diagram of Powling's "flat flame" apparatus.	28
6	Schematic diagram of an apparatus for determining burning velocities by the soap bubble method.	29
7	Diagram showing the relation between the burning velocity, (U_b), the speed in space of the combustion wave, (S_g), and the expansion ratio, (E), for the soap bubble method of determining the burning velocity.	30
8	Schematic diagram of the apparatus built and used to obtain the laminar burning velocity data presented in this thesis.	31
9	Diagram showing a typical inner-cone image, actual size, as observed on the tracing paper and the experimental method of obtaining data from this image.	32
10	Plot of laminar burning velocity in feet per second (U_b) versus volume percent of inert gas (I) for the inert gases Argon, Carbon Dioxide, Helium, and Nitrogen, where the molar ratio of acetylene to oxygen is constant for all mixtures and equal to 0.2, i. e., one-half the stoichiometric fuel/oxygen ratio.	33

Figure No.

Page No.

- | | | |
|----|--|----|
| 11 | Plot of laminar burning velocity in feet per second (U_b) versus volume percent of inert gas (I) for the inert gases Argon, Carbon Dioxide, Helium, and Nitrogen, where the molar ratio of acetylene to oxygen is constant for all mixtures and equal to 0.4, i. e., the stoichiometric fuel/oxygen ratio. | 34 |
| 12 | Plot of laminar burning velocity in feet per second (U_b) versus volume percent of inert gas (I) for the inert gases Argon, Carbon Dioxide, Helium, and Nitrogen, where the molar ratio of acetylene to oxygen is 0.8, i. e., twice the stoichiometric fuel/oxygen ratio. | 35 |
| 13 | Plot of laminar burning velocity in feet per second (U_b) versus volume percent of Argon (A) for the molar acetylene to oxygen ratios of 0.2, 0.4, and 0.8, i. e. one-half stoichiometric, stoichiometric, and twice stoichiometric fuel/oxygen ratios respectively. | 36 |
| 14 | Plot of laminar burning velocity in feet per second (U_b) versus volume percent of Carbon Dioxide (CO_2) for the molar acetylene to oxygen ratios of 0.2, 0.4, and 0.8, i. e., one-half stoichiometric, stoichiometric, and twice stoichiometric fuel/oxygen ratios respectively. | 37 |
| 15 | Plot of laminar burning velocity in feet per second (U_b) versus volume percent of Helium (He) for the molar acetylene to oxygen ratios of 0.2, 0.4, and 0.8, i. e., one-half stoichiometric, stoichiometric, and twice stoichiometric fuel/oxygen ratios respectively. | 38 |
| 16 | Plot of laminar burning velocity in feet per second (U_b) versus volume percent of Nitrogen (N_2) for the molar acetylene to oxygen ratios of 0.2, 0.4, and 0.8, i. e., one-half stoichiometric, stoichiometric, and twice stoichiometric fuel/oxygen ratios respectively. | 39 |